Scientific Research Publishing

Advances in Microbiology, 2022, 12, 649-670
https://www.scirp.org/journal/aim
ISSN Online: 2165-3410
ISSN Print: 2165-3402

Secalonic Acid and Benzoic Acid Analogues Exhibiting Cytotoxicity against Cancer Cells Isolated from *Claviceps yanagawaensis*

Yuji Doi[1], Daigo Wakana[1], Satoshi Kitaoka[2], Hisashi Takeda[1], Eiji Tanaka[3], Tomoo Hosoe[1*]

[1]Faculty of Pharmaceutical Sciences, Hoshi University, Tokyo, Japan
[2]Faculty of Pharmacy and Pharmaceutical Sciences, Josai University, Sakado, Japan
[3]Department of Environmental Science, Ishikawa Prefectural University, Nonoichi, Japan
Email: *hosoe@hoshi.ac.jp

How to cite this paper: Doi, Y., Wakana, D., Kitaoka, S., Takeda, H., Tanaka, E. and Hosoe, T. (2022) Secalonic Acid and Benzoic Acid Analogues Exhibiting Cytotoxicity against Cancer Cells Isolated from *Claviceps yanagawaensis*. *Advances in Microbiology*, **12**, 649-670.
https://doi.org/10.4236/aim.2022.1212045

Received: November 21, 2022
Accepted: December 17, 2022
Published: December 20, 2022

Abstract

The genus *Claviceps* (Clavicipitaceae) is noted for producing ergot alkaloids that cause ergotism. *Claviceps yanagawaensis*, a parasite of *Zoysia japonica* (family: Poaceae), has been isolated in Japan. Bioactivity screening showed that a methanol extract from a rice culture of *C. yanagawaensis* was cytotoxic to cancer cells. In our search for active substances, the new secalonic acid analogues (-)-5-*epi*-F-7 (**1**) and ergochrysin C (**2**) and a new benzoic acid analogue, dimethyl bigutol (**3**), were isolated along with the known compounds 3,4-dihydroxy-5-(3-methyl-2-buten-1-yl)benzoic acid (**4**) and methyl veratrate (**5**). The structures of **1** - **3** were elucidated by NMR, MS, and circular dichroism spectroscopy. MTT assays of **1** - **5** using cancer cell lines (HepG2, HL60, HT29, PANC-1, and T98G) showed that **1** - **4** exhibited cytotoxicity against cancer cells.

Keywords

Claviceps, Secalonic Acid, MTT Assay

1. Introduction

Members of the genus *Claviceps*, which includes parasitic fungi of mainly Poaceae and Cyperaceae families, produce ergot alkaloids in sclerotia (ergot) [1]. EAs (Ergot alkaloids) are the causative agent of ergotism, the main symptoms of which include convulsions and miscarriage [1]. Ergotism occurred frequently in medieval Europe and was feared as the "Fire of St. Anthony" [2]. In modern times, ergotism outbreaks were reported in India in 1975 (caused by *C. fusifor-*

mis) and Ethiopia in 2001 (caused by *C. purpurea*) [3] [4]. Since the Middle Ages, ergotism outbreaks have caused significant health problems worldwide. Ergotism outbreaks have also affected Japan, and many miscarriages occurred in 1943 due to ingestion of bread made from bamboo grass seeds [5]. In livestock production, ergotism symptoms have also been reported in calves [6].

Our studies have focused on the genus *Claviceps* in Japan. *Claviceps yanagawaensis*, a parasite of *Zoysia japonica* (family: Poaceae), has been isolated only in Japan [7] [8]. Bioactivity screening showed that a methanol extract of *C. yanagawaensis* cultured on rice was cytotoxic to HepG2 cells. Although ergot alkaloids are cytotoxic to cancer cells, we previously reported that *C. yanagawaensis* does not produce ergot alkaloids in artificial culture [9] [10]. To date, no detailed metabolite studies have been reported for *C. yanagawaensis*. Therefore, we screened for cytotoxic components other than EAs using methanol extracts of rice cultures of *C. yanagawaensis*. A new secalonic acid analogue, (-)-5-*epi*-F-7 (**1**), ergochrysin C (**2**), and a new benzoic acid analogue, dimethyl bigutol (**3**), were isolated, along with the known compounds 3,4-dihydroxy-5-(3-methyl-2-buten-1-yl)benzoic acid (**4**) and methyl veratrate (**5**) (Figure 1 and Figure S1). In this paper, we report the structures of **1**-**3** and the cytotoxicity of **1** - **5** against five cancer cell lines (HepG2, HL60, HT29, PANC-1, and T98G) determined using the 3-[4,5-dimethylthiazol-2-yl]-2,5-diphenyl-tetrazolium bromide (MTT) assay.

2. Materials and Methods

2.1. Experimental Instruments

HPLC analysis was performed using an 1100 series HPLC system (binary pump: G1312A, auto sampler: A1329A, column compartment: G1316A, UV detector: G1314A, Agilent Technologies, Inc., Santa Clara, CA, USA) equipped with an

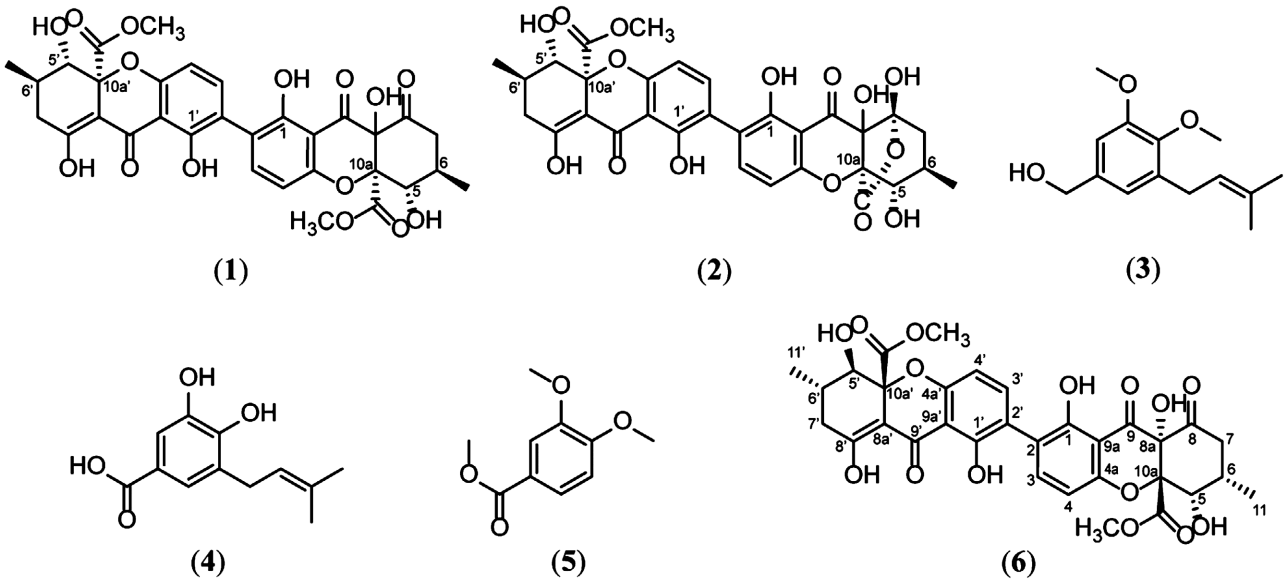

Figure 1. Structures of compounds **1** - **6**.

Inertsil ODS-3 column (3 μm, 2.1 × 150 mm) (GL Science Inc., Tokyo, Japan). Open column chromatography for compound isolation was performed using 100 g of Sephadex LH-20 (GE Healthcare, Chicago, IL, USA) in a 3.5 × 80 cm glass column. Preparative MPLC was performed on a Shimadzu LC-20AT and SPD-10AV instrument equipped with an ULTRA PACK ODS-S-50B column (50 μm, 26 × 300 mm) (Yamazen Corp., Osaka, Japan). Preparative HPLC was performed on a Shimadzu LC-20AT and SPD-10AV instrument equipped with a GL Science InertSustain C18 column (5 μm, 10 × 250 mm). NMR spectra were recorded on an ECA-600II instrument (^{1}H: 600.17 MHz; ^{13}C: 150.91 MHz) (JEOL, Tokyo, Japan). Chemical shifts for ^{1}H- and ^{13}C-NMR are given in parts per million (δ) relative to residual solvent signals ([δ_H 7.26]/[δ_C 77.0] for $CDCl_3$, [δ_H 2.49]/[δ_C 39.5] for DMSO-d_6 as internal standards). Mass spectra were measured on a JEOL JMS-T100LP or JMS-700. Circular dichroism (CD) spectra were recorded on a J-820 spectropolarimeter (Jasco). Liquid cultures were fermented in a Taitec Bio-Shaker BR-300LF (Taitec Corp., Saitama, Japan). Rice cultures were fermented in a Sanyo MIR-554 incubator (Sanyo Electric Co., Ltd., Osaka, Japan).

2.2. Material

The *C. yanagawaensis* MAFF 247556 isolate was obtained from ears of *Zoysia japonica*.

2.3. Fermentation

Claviceps yanagawaensis was pre-cultured on potato dextrose agar (PDA, Nissui Pharmaceutical Co., Ltd., Tokyo, Japan). Fermentation was conducted using M102 medium (sucrose 30 g, malt extract 20 g, peptone 2 g, yeast extract 1 g, $MgSO_4$-$7H_2O$ 0.5 g, KCl 0.5 g, KH_2PO_4 1.0 g, purified water 1 L, NaOH [pH 6.0]) and rice medium (rice: 750 g, tap water: 450 mL).

First, *C. yanagawaensis* was pre-cultured on PDA for 21 days at 25˚C, after which two pieces of cultured agar (1 × 2 cm^2) were transferred into 500-mL Erlenmeyer flasks containing 200 mL of M102 medium and grown at 25˚C with shaking at 150 rpm for 7 days. Next, 10-mL aliquots of cultured M102 medium were transferred into 500-mL Roux flasks containing rice medium (each flask contained 150 g of medium as dry rice) and grown at 25˚C for 28 days.

2.4. Extraction and Isolation

Each rice culture of *C. yanagawaensis* was extracted with 2.5 L of methanol, and then the methanol extract was evaporated to dryness in a vacuum evaporator. The crude methanol extract (9.83 g) was suspended in 300 mL of water and extracted three times with an equal volume of ethyl acetate. The resulting ethyl acetate extract (2.1 g) was obtained by evaporation under vacuum, suspended in 300 mL of *n*-hexane, and extracted three times with an equal volume of acetonitrile. The solvent was removed under vacuum, and the acetonitrile extract (1461.5

mg) was separated into 11 fractions (A-K) by open column chromatography using Sephadex LH-20. The mobile phases were *n*-hexane:chloroform (1:4; 200 mL), chloroform:acetone (3:2; 200 mL and 1:4; 200 mL), acetone (200 mL), and MeOH (500 mL). Fraction E (136.4 mg) was purified by HPLC on an ODS column eluted with 50% acetonitrile to obtain **1** (3.5 mg) as a yellow amorphous powder. Fraction F (135.3 mg) was separated by MPLC on an ODS column eluted with 50% acetonitrile to obtain 7 fractions. Fraction F-5 (19.3 mg) was purified by HPLC on an ODS column eluted with 45% acetonitrile to obtain **2** (2.1 mg) as a yellow amorphous powder. Fraction C (77.5 mg) was purified by HPLC on an ODS column eluted with 50% acetonitrile to obtain **3** (27.3 mg) as a colorless oil. Fraction I (43.4 mg) was separated by MPLC on an ODS column eluted with 50% acetonitrile to obtain 7 fractions. Fraction I-5 (10.7 mg) was purified by HPLC on an ODS column eluted with 50% acetonitrile to obtain 3,4-dihydroxy-5-(3-methyl-2-buten-1-yl)benzoic acid (**4**; 7.9 mg) as a white amorphous powder [11]. Fraction B (162.6 mg) was separated by MPLC on an ODS column eluted with 50% acetonitrile to obtain 4 fractions. Fraction B-2 (34.6 mg) was purified by HPLC on an ODS column eluted with 50% acetonitrile to obtain methyl veratrate (**5**; 16.2 mg) as a white amorphous powder [12]. The absence of EAs in the extracts was confirmed by HPLC analysis (data not shown).

Compound **1**: yellow amorphous powder. $[\alpha]_D^{24}$ −351.3 (c 0.1, $CHCl_3$). UV (MeOH) λ_{max} 204 nm (logε 5.57), 335 (logε 5.38). ^{1}H- and ^{13}C-NMR data, see Table 1. HR-ESI-MS (negative ion) *m/z* $[M-H]^-$ 653.1514 (calcd for $C_{32}H_{29}O_{15}$: 653.1506).

Compound **2**: yellow amorphous powder. $[\alpha]_D^{24}$ −222.02 (c 0.1, $CHCl_3$). UV (MeOH) λ_{max} 204 nm (logε 5.49), 335 (logε 5.23). ^{1}H- and ^{13}C-NMR data, see Table 1. HR-ESI-MS (negative ion) *m/z* $[M-H]^-$ 639.1328 (calcd for $C_{31}H_{27}O_{15}$: 639.1350).

Compound **3**: colorless oil. UV (MeOH) λ_{max} 206 nm (logε 4.69), 273 (logε 0.67). ^{1}H- and ^{13}C-NMR data, see Table 2. HR-EI-MS (positive ion) *m/z* $[M]^+$ 236.1413 (calcd for $C_{14}H_{20}O_3$: 236.1412).

2.5. Cell Lines and Cell Culture

Human hepatoma cells (HepG2) were obtained from the National Institutes of Bio-medical Innovation, Health, and Nutrition (Osaka, Japan). Human promyelocytic leukemia cells (HL60), human pancreatic carcinoma cells (PANC-1), and human glioblastoma multiforme tumor cells (T98G) were obtained from Riken BioResource Research Center (Ibaraki, Japan). Human colon adenocarcinoma cells (HT29) were obtained from KAC Co., Ltd. (Kyoto, Japan). Cells were cultured in DMEM (Nacalai Tesque, Inc., Kyoto, Japan) or RPMI 1640 (Nacalai Tesque, Inc.) supplemented with 10% heat-inactivated fetal bovine serum (Merck, Darmstadt, Germany) and 1% Antibiotic-Antimycotic Mixed Stock Solution (Nacalai Tesque, Inc.) at 37˚C in a humid incubator containing ambient air supplemented with 5% CO_2.

2.6. Cell Viability Assay

Cell viability was measured using an MTT Cell Count kit (Nacalai Tesque, Inc.) according to the manufacturer's instructions. Briefly, cells were seeded in a 96-well plate at 5.0×10^3 cells per well; each experiment was performed with four replicates. After 48 h, the growth medium was replaced with fresh medium supplemented with test compounds (at concentrations ranging from 6.25 to 100 μM), and the plates were cultured for another 72 h. Next, 10 μL of MTT solution was added to each well, and the plates were incubated at 37˚C for 3 h and then treated with 100 μL/well of solubilization solution to dissolve the formazan crystals. The absorbance at 570 nm was measured using a microplate reader (As One Corp., Osaka, Japan). Cell viability is expressed as the relative percentage of absorbance in the experimental groups normalized to that of the negative control (no added compound) group; where appropriate, outliers were excluded based on identification using the Smirnov-Grubbs test.

2.7. Statistical Analysis

Statistical analysis was performed using the multcomp package in R, version 4.1.0 [13]. Where appropriate, values are expressed as mean ± standard deviation (SD). Comparisons to the respective negative controls were conducted using Dunnett's multiple comparisons test. Values of $p < 0.05$ were considered statistically significant.

3. Results

3.1. Characterization of Isolated Compounds

Compound **1** {$[\alpha]_D^{24}$ −351.3 (c 0.1, $CHCl_3$)} was obtained as a yellow amorphous powder solid. Compound **1** was revealed to have the molecular formula $C_{32}H_{30}O_{15}$ [*m/z* 653.1514, $[M\text{-}H]^-$, calcd 653.1506] based on HR-ESI-MS data. The ^{1}H-NMR spectrum of **1** in $CDCl_3$ (**Table 1**) showed four doublet aromatic protons [δ_H 7.57 (d, J = 8.7 Hz), 7.47 (d, J = 8.7 Hz), 6.68 (d, J = 8.7 Hz), 6.63 (d, J = 8.7 Hz)] and suggested the presence of two benzene rings with ortho coupling. The ^{1}H-NMR spectrum also showed two doublet methyl protons [δ_H 1.22 (d, J = 6.6 Hz) and δ_H 1.17 (d, J = 5.8 Hz)], two oxygen-bearing methyl protons (δ_H 3.68 and 3.72), and two oxygen-bearing methine protons [δ_H 4.50 (d, J = 10.7 Hz) and δ_H 3.93 (d, J = 11.6 Hz)]. The ^{13}C-NMR spectrum showed three ketone carbonyl (δ_C 198.9, 191.8, 187.1) and three sp^3 quaternary carbons, four sp^3 methyl carbons, two sp^3 methylene carbons, two sp^3 methine carbons, two oxygen-bearing sp^3 methine carbons, and 16 sp^2 carbons (estimated benzene rings, an olefin carbon, an oxygen-bearing olefin carbon or ester carbons).

Next, the planar structure of **1** was elucidated through detailed analyses of 2D NMR data, including ^{1}H-^{1}H correlation spectroscopy (COSY), heteronuclear single quantum coherence (HSQC), and heteronuclear multiple bond correlation (HMBC) spectra in $CDCl_3$ (**Figure 2** and **Figures S2-S6**). The ^{1}H-^{1}H COSY correlations for H-3 (δ_H 7.57)/H-4 (δ_H 6.68) and HMBC correlations from H-3 to

Table 1. ^{1}H- and ^{13}C-NMR spectral data of compounds **1**, **2**, and F-7 (**6**) in $CDCl_3$.

NMR data position	**1**		**2**		F-7 (**6**) [14]	
	δ_C	δ_H (J in Hz)	δ_C	δ_H (J in Hz)	δ_C	δ_H (J in Hz)
1	160.6		160.6		159.3	
2	118.5		119.0		119.1	
3	141.4	7.57 (d, 8.7)	144.5	7.66 (d, 8.3)	140.4	7.50 (d, 8.5)
4	107.1	6.68 (d, 8.7)	107.8	6.77 (d, 8.3)	107.6	6.61 (d, 8.4)
4a	157.4		157.8		158.4	
5	74.0	4.50 (d, 10.7)	71.9	4.22 (d, 9.9)	75.0	4.38 (brs)
6	32.0	2.07 (m)	32.2	1.82 (m)	31.3	2.04-1.99 (m)
7	43.4	2.49 (dd, 15.3, 5.8) 2.94 (dd, 15.3, 12.4)	36.4	2.14 (dd, 14.5, 6.6) 2.23 (dd, 14.5, 12.4)	39.7	2.37-2.33 (s) 3.17 (dd, 15.1, 13.6)
8	198.9		107.1		198.7	
8a	71.7		72.0		72.5	
9	191.8		196.3		190.3	
9a	106.6		107.2		106.9	
10a	89.4		86.1		86.2	
11	18.4	1.22 (d, 6.6)	17.4	1.25 (d, 6.6)	18.0	1.21 (d, 6.6)
12	167.9		166.2		168.5	
13	53.5	3.68 (s)			53.2	3.69 (s)
OH-1		11.77 (s)		11.40 (s)		11.71 (s) or 11.88 (s)
OH-5						
OH-8a		5.09 (s)		6.62 (s)		
1’	159.2		159.2		160.2	
2’	117.4		116.9		117.7	
3’	140.4	7.47 (d, 8.7)	140.0	7.42 (d, 8.3)	140.3	7.46 (d, 8.5)
4’	107.7	6.63 (d, 8.7)	107.8	6.64 (d, 8.3)	106.9	6.60 (d, 8.4)
4a’	158.3		158.6		156.7	
5’	76.9	3.93 (d, 11.6)	76.9	3.93 (d, 11.6)	77.2	3.93 (d, 11.0)
6’	29.2	2.42 (m)	29.2	2.43 (m)	29.7	2.47-2.37 (m)
7’	36.2	2.32 (dd, 19.4, 10.7) 2.74 (dd, 19.4, 6.6)	36.2	2.32 (dd, 19.4, 9.9) 2.75 (dd, 19.4, 6.6)	36.3	2.33-2.29 2.74 (dd, 18.8, 5.9)
8’	177.5		177.8		177.6	
8a’	101.5		101.4		101.5	
9’	187.1		187.0		187.1	
9a’	106.9		106.9		106.9	
10a’	84.8		84.3		84.2	

Continued

11’	18.0	1.17 (d, 5.8)	18.0	1.18 (d, J = 6.6)	17.1	1.17 (d, 6.3)
12’	170.3		170.2		170.3	
13’	53.3	3.72 (s)	53.3	3.74 (s)	53.8	3.72 (s)
OH-1’		11.73 (s)		11.74 (s)		
OH-5’						11.71 (s) or 11.88 (s)
OH-8’		13.76 (s)		13.73 (s)		

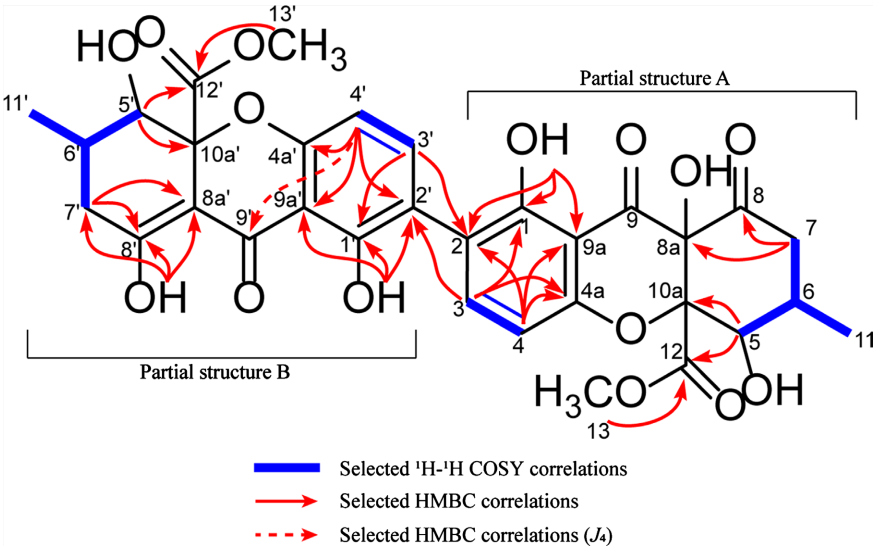

Figure 2. Key ^{1}H-^{1}H COSY and HMBC correlations of compound **1**.

C-1 (δ_C 160.6) and C-4a (δ_C 157.4), from H-4 to C-2 (δ_C 118.5), C-4a and C-9a (δ_C 106.6), and from OH-1 (δ_H 11.77) to C-1, C-2, and C-9a suggested a benzene ring with a hydroxy group at the 1-position and an oxygen attached at the 4a-position. The ^{1}H-^{1}H COSY correlations for H-11 (δ_H 1.22)/H-6 (δ_H 2.07), H-6 (δ_H 2.07)/H-7(δ_H 2.49, 2.94)/H-5 (δ_H 4.50) and HMBC correlations from H-7 to C-8 (δ_C 198.9) and C-8a (δ_C 71. 7) and from H-5 to C-10a (δ_C 89.4) suggested a cyclohexanone ring with a methyl group at the 6-position, a hydroxy group at the 5-position, and a carbonyl group at the 8-position. In addition, HMBC correlation from the H-5 methine and H-13 methyl to C-12 (δ_C 167.9) suggested partial structure A with a carboxymethyl group at the 10a-position (**Figure 2**).

Similarly, the ^{1}H-^{1}H COSY correlations for H-3’ (δ_H 7.47)/H-4’ (δ_H 6.63) and HMBC correlations from H-3’ to C-1’ (δ_C 159.2), from H-4’ to C-2’ (δ_C 117.4), C-4a’ (δ_C 158.3), C-9a’ (δ_C 106.9), and C-9’ (δ_C 187.1) and from OH-1’ (δ_H 11.73) to C-1’, C-2’, and C-9a’ suggested another benzene ring with a hydroxy group at the 1’-position and an oxygen attached at the 4a’-position. The ^{1}H-^{1}H COSY correlations for H-11’ (δ_H 1.17)/H-6’ (δ_H 2.42), H-6’/H-7’ (δ_H 2.32, 2.74), and H-5’ (δ_H 3.93) and HMBC correlations from H-7’ to C-8’ (δ_C 177.5) and C-8a’ (δ_C 101.5), from H-5’ to C-10a’ (δ_C 84.8), and from OH-8’ (δ_H 13.76) to C-7’ (δ_C 36.2), C-8’, and C-8a’ suggested a cyclohexene ring with a methyl group at the

6'-position and a hydroxy group at the 5'- and 8'-positions. In addition, HMBC correlation from the H-5' methine and H-13' methyl to C-12' (δ_C 170.3) suggested partial structure B. The HMBC correlations from H-3 to C-2' and from H3' to C-2 suggested a 2-2' bond between partial structures A and B.

These results and UV spectra (λ_{max} 204, 264 and 335 nm) suggested that **1** is a secalonic acid analogue as a dimer of tetrahydroxanthone derivatives. The ^{1}H- and ^{13}C-NMR data indicated that **1** was similar to the secalonic acid analogue F-7 (**6**), except for the coupling constant at the 5-position (**1**: d, 10.7 Hz, F-7 (**6**): brs). Therefore, we considered **1** to be a stereoisomer of F-7 (**6**) (**Figure 2**) [14].

The configuration of **1** was also examined. The 5'-H/6'-H coupling constant of **1** was 11.6 Hz, similar to that of F-7 (**6**, 11.0 Hz), and these two hydrogens had a *trans*-diaxial configuration, but 5-H/6-H differed significantly from that of F-7 (**6**; brs) at 10.7 Hz. Thus, the 5-H/6-H configuration of **1** was suggested as *trans*, different from that of F-7 (**6**).

Next, we examined the configuration at the 10a- and 10a'-positions of **1**. In the case of secalonic acids, it has been reported that the Cotton around 330 nm in the CD spectrum correlates with the configuration at the 10a- and 10a'-positions [14] [15] [16] [17] [18]. The CD spectrum of **1**, which showed a negative Cotton around 333 nm, suggested that **1** has a configuration of 10a*R* and 10a'*S*, which differs from that of F-7 (**6**; 10a*S*, 10a'*R*) (**Figure 3**).

The configurations at positions 5, 6, and 10a and 5', 6', and 10a' of **1** were estimated from the biosynthetic reaction of secalonic acids. The tetrahydroxanthone skeleton, the monomer unit of secalonic acids, is formed by spontaneous cyclization of the biosynthetic intermediate diphenylmethanone analogue A (**Figure S7**). During this spontaneous cyclization reaction, the carboxymethyl group at position 10a and the methyl group at position 11 are enantioselectively placed in the *trans* configuration due to 1,3-axial pseudoaxial interaction [19]

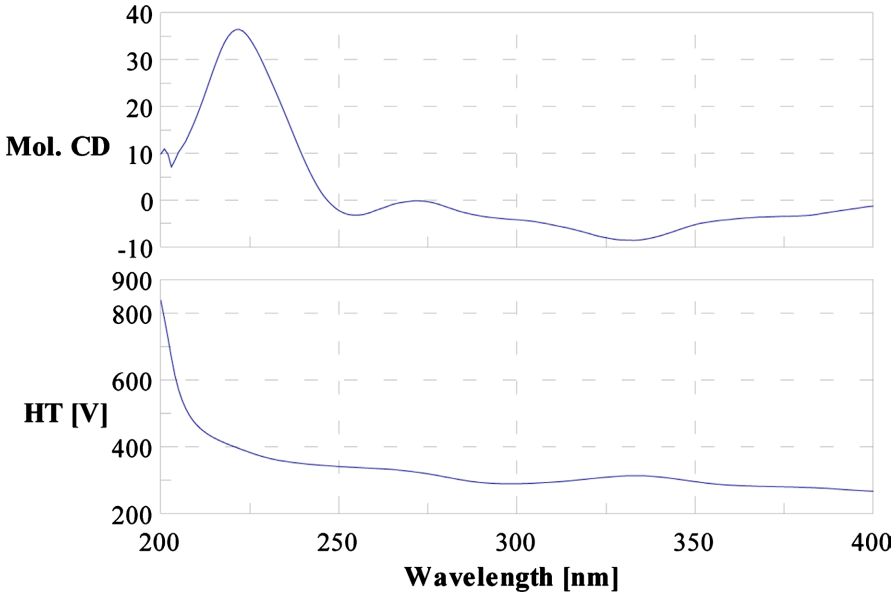

Figure 3. CD spectrum of compound **1** in methanol.

[20]. Therefore, the configuration of **1** was 5*S*, 6*R*, 10a*R*, 5'*S*, 6'*R*, and 10a'*S*, and the structure of **1** was suggested to be (-)-5-*epi*-F-7 (Figure 1).

Compound **2** {$[\alpha]_D^{24}$ −222.02 (c 0.1, $CHCl_3$)} was obtained as a yellow amorphous powder solid. Compound **2** was revealed to have the molecular formula $C_{31}H_{28}O_{15}$ [*m/z* 639.1328, $[M-H]^-$, calcd 639.1350] by HR-ESI-MS data. From the molecular formula and UV spectra (λ_{max} 204 and 335 nm), **2** was estimated to be a secalonic acid analogue with a molecular weight lower by CH_2 than compound **1**. Comparing ^{1}H- and ^{13}C-NMR spectra in $CDCl_3$ (Table 1, Figure 4 and Figures S8-S12) with those of **1**, the 13-position methyl disappeared, and the carbon at the 8-position shifted downfield. Therefore, the structure of **2** was suggested to be a lactone ring formed between positions 10a and 8 of **1**. This result was supported by detailed analysis of the 2D NMR spectra (Figure 4).

The configurations at 5-H/6-H and 5'-H/6'-H of **2** were *trans*-diaxial due to similarity to the coupling constants of **1**. The CD spectra of **2** showed a negative Cotton around 333 nm (Figure 5). The configuration at the chiral center of **2** was estimated as 5*S*, 6*R*, 8*R*, 10a*R*, 5'*S*, 6'*R*, and 10a'*S*, and the structure of **2** was suggested as shown in Figure 1.

Compound **3** was obtained as a colorless oil. Compound **3** was revealed to have the molecular formula $C_{14}H_{20}O_3$ [*m/z* 236.1413, $[M]^+$, calcd. 236.1412] based on HR-EI-MS data. The ^{1}H-NMR spectrum of **3** in DMSO-d_6 (Table 2) showed two doublet aromatic protons [δ_H 6.81 (d, J = 1.4 Hz), 6.66 (d, J = 1.4 Hz)] and suggested the presence of a 1,3,4,5-tetrasubstituted benzene ring with meta coupling. One olefine proton (δ_H 5.18) suggested the presence of a trisubstituted olefinic moiety. Two oxygen-bearing methyl protons (δ_H 3.65 and 3.75) suggested two methoxy groups. The ^{1}H-NMR spectrum also showed two broadened singlet methyl protons (δ_H 1.67 and δ_H 1.68), one oxygen-bearing methylene proton [δ_H 4.37 (d, J = 5.5 Hz)], and a doublet methylene-attached olefin [δ_H 3.23 (d, J = 7.6 Hz)]. The ^{13}C-NMR spectrum showed two sp^3 methyl carbons, two oxygen-bearing sp^3 methyl carbons, one sp^3 methylene carbon and one oxygen-bearing sp^3 methylene carbon, and eight sp^2 carbons (estimating a

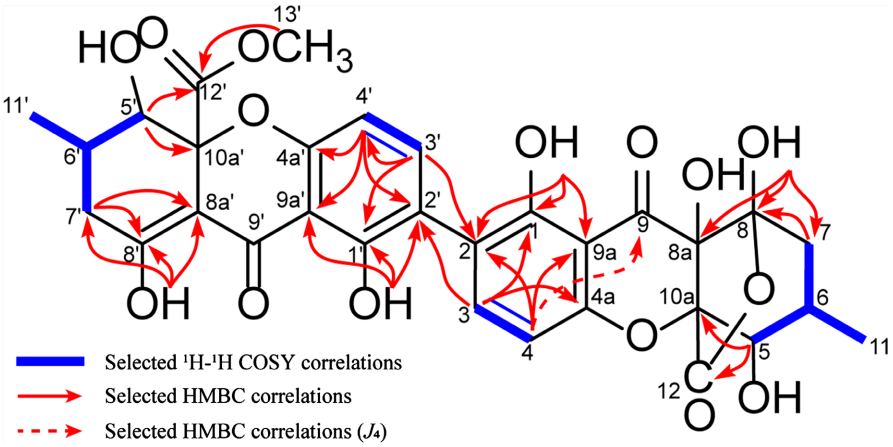

Figure 4. Key ^{1}H-^{1}H COSY and HMBC correlations of compound **2**.

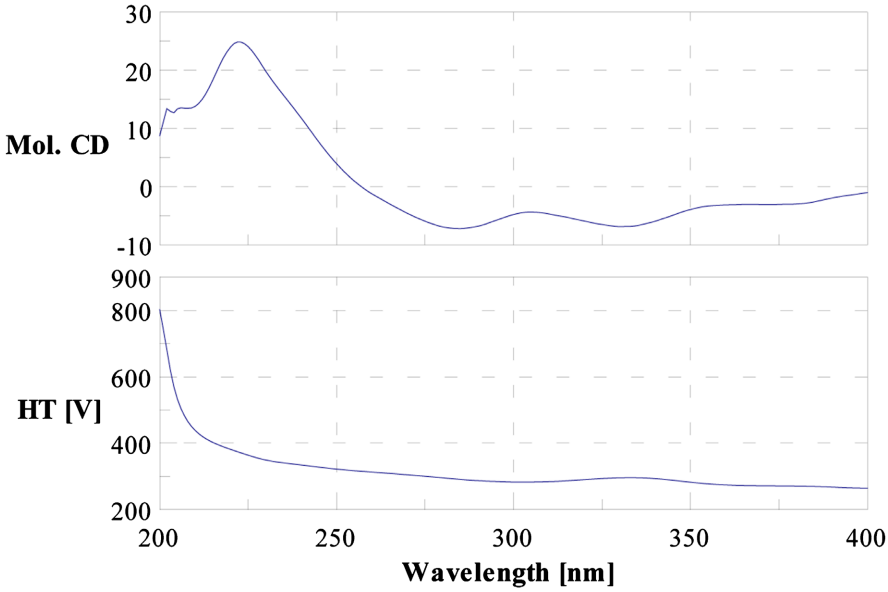

Figure 5. CD spectra of compound **2** in methanol.

Table 2. ^{1}H- and ^{13}C-NMR spectral data of compound **3** in DMSO-d_6.

NMR data position	**3**	
	δ_C	δ_H (j in Hz) in DMSO-d_6
1	134.1	
2	145.0	
3	152.1	
4	108.9	6.81 (d, 1.4)
5	138.1	
6	119.2	6.66 (d, 1.4)
7	28.1	3.23 (d, 7.6)
8	123.2	5.18 (m)
9	131.2	
10	25.5	1.67 (brs)
11	17.6	1.68 (brs)
12	62.9	4.37 (d, 5.5)
13	55.5	3.75 (s)
14	59.8	3.65 (s)
OH-12		5.09 (t, 5.5)

benzene ring and two olefin carbons).

The gross structure of **3** was elucidated through detailed analyses of 2D NMR data, including ^{1}H-^{1}H COSY, HSQC, and HMBC spectra in DMSO-d_6 (Figure 6 and Figures S13-S17). The ^{1}H-^{1}H COSY correlations for OH-12 (δ_H 5.09)/H-12

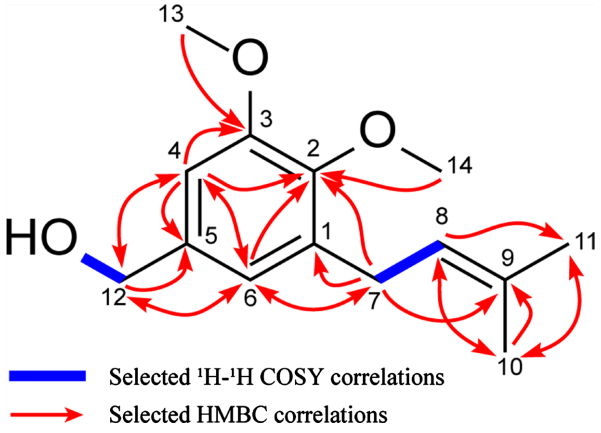

Figure 6. Key ^{1}H-^{1}H COSY and HMBC correlations of compound **3**.

(δ_H 4.37) and HMBC correlations from H-4 (δ_H 6.81) to C-2 (δ_C 145.0), C-3 (δ_C 152.1), C-5 (δ_C 138.1), C-6 (δ_C 119.2), and C-12 (δ_C 62.9), from H-6 (δ_H 6.66) to C-2, C-4 (δ_C 108.9), and C-12, and from H-12 to C-4, C-5, and C-6 suggested a benzene ring with a hydroxy methyl group at the 5-position. The HMBC correlations from H-13 (δ_H 3.75) to C-3 and from H-14 (δ_H 3.65) to C-2 suggested methoxy groups at the 2- and 3-positions. The ^{1}H-^{1}H COSY correlations for H-7 (δ_H 3.23)/H-8 (δ_H 5.18) and HMBC correlations from H-11 (δ_H 1.68) to C-10 (δ_C 25.5) and from H-10 (δ_H 1.67), C-8 (δ_C 123.2), C-9 (δ_C 131.2), and C-11 (δ_C 17.6) suggested the presence of a dimethylallyl group. The HMBC correlations from H-7 (δ_H 3.23) to C-1 (δ_C 134.1), C-2, and C-6 and from H-6 to C-7 (δ_C 28.1) suggested that the dimethylallyl group was attached at the 1-position. Therefore, the structure of **3** was determined as a 3-methoxy derivative (Figure 1) of methyl bigutol isolated from the mycoparasite *Verticillium biguttatum* (Table S1) [21].

3.2. Effect of the Compounds on the Viability of Cancer Cell Lines

MTT assays were performed using HepG2, HL60, HT29, PANC-1, and T98G cell lines to investigate the cytotoxicity of the isolated compounds against cancer cells (Figure 7). Compound **1** decreased the viability of HepG2, HT29, PANC-1, and T98G at 100 μM, especially T98G at 12.5 μM in a concentration-dependent manner. Compound **2** slightly decreased the viability in HepG2 and PANC-1 cells at 100 μM. Compound **3** decreased the viability of HepG2, HL60, HT29, and PANC-1 at 100 μM, especially HL60 at 6.25 μM in a concentration-dependent manner. Compound **4** decreased the viability of HepG2, HL60, and PANC-1 cells at 100 μM, reducing the viability of PANC-1 cells to <50% relative to control cells. Compound **5** at 100 μM did not affect the viability of any of the cancer cell lines examined.

4. Discussion

In this study, secalonic acid analogues **1** and **2** and benzoic acid analogues **3** - **5** were isolated from methanol extracts of *C. yanagawaensis*. These compounds

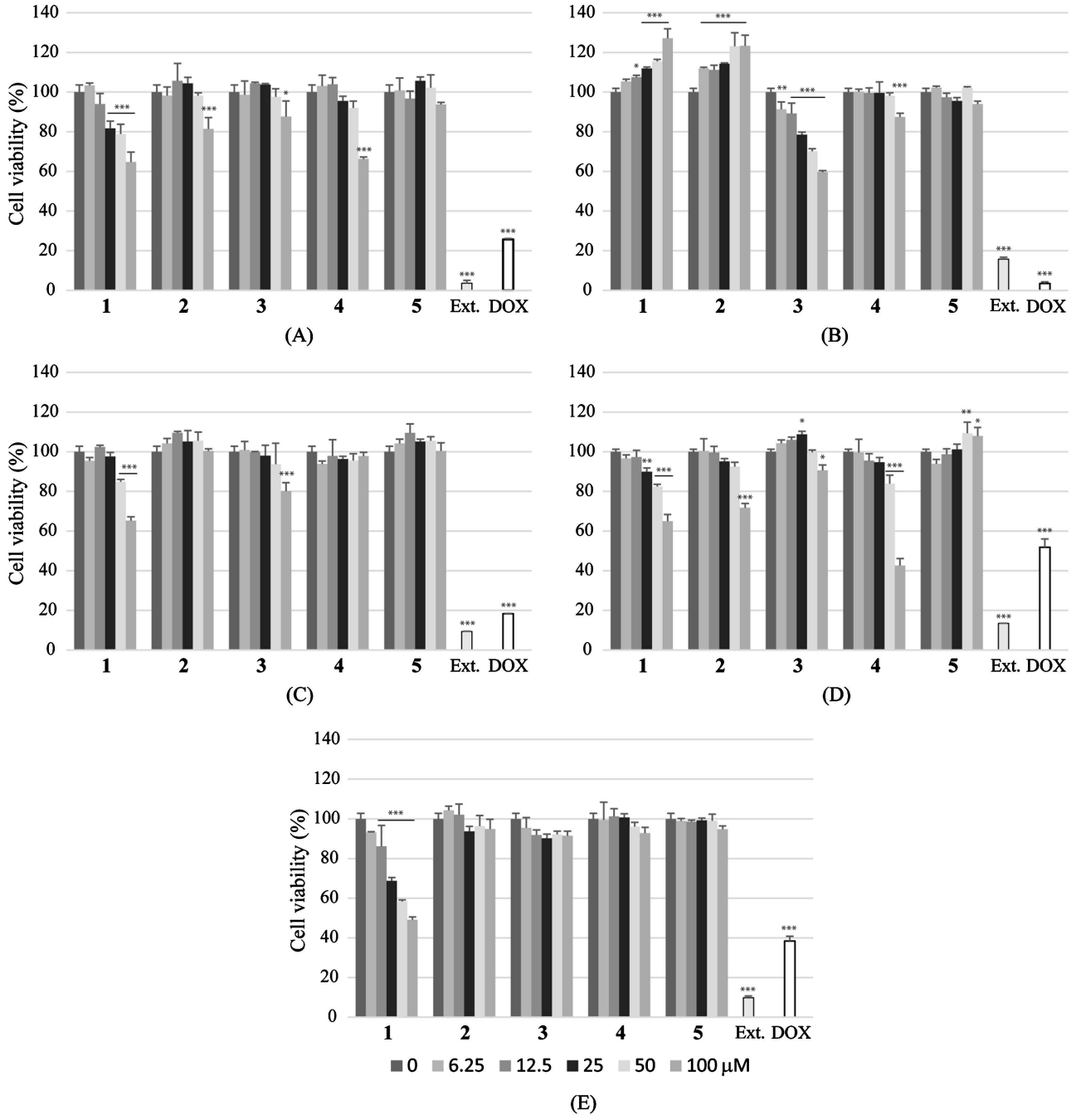

Figure 7. Effect of isolated compounds (**1** - **5**) and the methanol extracts (Ext.) on the viability of cancer cells, as assessed using the MTT assay. The methanol extract of *C. yanagawaensis* cultured on rice (Ext., 400 μg/mL) and Doxorubicin (DOX, 0.5 μM) were employed as a positive (cell death–inducing) control. Data are shown as the mean ± SD (n = 4). Comparisons with the negative control (no added compound) were performed using Dunnett's multiple comparisons test. *$p < 0.05$, **$p < 0.01$, ***$p < 0.001$. Conditions without an asterisk exhibited no significant difference. (A) HepG2; (B) HL60; (C) HT29; (D) PANC-1; (E) T98G.

exhibited cytotoxicity against several cancer cell lines, including HepG2, HT29, PANC-1, and T98G cells.

Secalonic acids are structurally diverse, and polyketide synthases are involved in biosynthesis [19] [22]. Compound **1** has the same planar structure as F-7 (**6**) isolated from *Aspergillus aculeatus* MBT 102, but detailed analysis of NMR and

CD spectra suggested that the configuration of compound **1** differs from that of F-7 (**6**). Secalonic acids with dimeric tetrahydroxanthone derivative structures are produced by fungi in the *Aspergillus*, *Pyrenochaeta*, and other genera, in addition to *Claviceps*. The monomers (blennolide A, B, [-]-blennolide A, B, and their derivatives with chiral carbons at C-5, C-6, and C-10a) constituting the dimer differ according to the genus of the producing fungi (**Figure S18**) [23]. Secalonic acids produced by *Aspergillus* and *Claviceps* species commonly produce blennolide A (5*S*, 6*S*, 10a*R*) as a component, whereas *Claviceps* and *Pyrenochaeta* commonly produce (-)-blennolide B (5*S*, 6*R*, 10a*S*), *Aspergillus* produces blennolide B (5*R*, 6*S*, 10a*R*), and *Pyrenochaeta* produces (-)-blennolide A (5*R*, 6*R*, 10a*S*) [19] [20] [24]. Therefore, *Aspergillus* produces secalonic acid B; blennolide A dimer, secalonic acid D; blennolide B dimer and secalonic acid F; blennolide A and blennolide B dimer (**Figure S18**). In contrast, *Claviceps* produces secalonic acid A: (-)-blennolide B dimer, secalonic acid B; blennolide A dimer, secalonic acid C; blennolide A and (-)-blennolide B dimer (**Figure S18**). The conformation of **1** was found to be 5*S*, 6*R*, 8*R*, 10a*R*, 5'*S*, 6'*R*, and 10a'*S*, the same conformation as the dimer of (-)-blennolide B and its derivatives, in agreement with the abovementioned studies.

Compound **2** is similar to **1** and estimated to have the same 5*S*, 6*R*, 10a*R*, 5'*S*, 6'*R*, and 10a'*S* configuration based on NMR and CD spectra. Secalonic acid analogues with a lactone ring have been reported, including ergoflavin, ergochrysin A, and ergochrysin B, and secalonic acid analogues with a lactone ring and hydroxy group attached at the 8-position, as in **2**, were isolated from *Claviceps* by Lünne *et al.* [17]. Lactone cyclization of ergoflavin, ergochrysin A, and ergochrysin B is predicted to proceed via the addition of H_2O to the 8-8a olefin and condensation of the hydroxy group at the 8-position with the carboxymethyl group at the 10a-position (**Figure S19**) [25] [26]. In contrast, it is expected that the lactone ring of **2** cyclizes in a different manner and has a hydroxy group attached at the 8-position.

MTT assay results showed that **1** was cytotoxic to T98G cells, whereas **3** was cytotoxic to HL60 cells and **4** to PANC-1 cells (**Figure 7**). The secalonic acid F analogue F-7 (**6**) has been shown to induce apoptosis and inhibit microtubule formation in MDA-MB-231 human breast cancer cells [14]. Secalonic acid A inhibits topoisomerases I and II in CCF-STTG-1 glioma cells and induces apoptosis in Jurkat human T-cell leukemia-derived cells [17] [27]. In this study, secalonic acid (-)-5-*epi*-F-7 (**1**), isolated from *C. yanagawaensis*, was shown to be cytotoxic to cancer cells and therefore expected to exhibit similar activity.

5. Conclusion

Novel cytotoxic secalonic acid analogues (-)-5-*epi*-F-7 (**1**), ergochrysin C (**2**), and dimethyl bigutol (**3**) were isolated from methanol extracts of *C. yanagawaensis* rice cultures. These results highlight the potential of members of the genus *Claviceps* to produce bioactive substances. We plan to carry out further

investigations of ergot alkaloids and other bioactive substances produced by *C. yanagawaensis* sclerotia to better characterize the possibility of poisoning in nature.

Fund

This work was supported by JSPS KAKENHI grant number 16K07238.

Conflicts of Interest

The authors declare no conflicts of interest regarding the publication of this paper.

References

[1] Haarmann, T., Rolke, Y., Giesbert, S. and Tudzynski, P. (2009) Ergot: From Witchcraft to Biotechnology. *Molecular Plant Pathology*, **10**, 563-577. https://doi.org/10.1111/j.1364-3703.2009.00548.x

[2] Lee, M.R. (2009) The History of Ergot of Rye (*Claviceps purpurea*) I: From Antiquity to 1900. *Journal of the Royal College of Physicians of Edinburgh*, **39**, 179-184.

[3] Krishnamachari, K.A. and Bhat, R.V. (1976) Poisoning by Ergoty Bajra (*Pearl millet*) in Man. *Indian Journal of Medical Research*, **64**, 1624-1628.

[4] Urga, K., *et al.* (2002) Laboratory Studies on the Outbreak of Gangrenous Ergotism Associated with Consumption of Contaminated Barley in Arsi, Ethiopia. *Ethiopian Journal of Health Development*, **16**, 317-323. https://doi.org/10.4314/ejhd.v16i3.9800

[5] Szuki, N. (2018) A Viewpoint Regarding the Use of Coix Seed During Pregnancy. *Japanese Journal of Complementary and Alternative Medicine*, **15**, 141-151. (In Japanese) https://doi.org/10.1625/jcam.15.141

[6] Sakamoto, R., *et al.* (2010) Bakkaku arukaroido tyudoku wo utagatta shitaneshi no kousi no 2 syourei [Two Cases of Calf with Limb End Necrosis Suspected to Be due to Ergot Alkaloids Poisoning]. *Journal of the Hokkaido Veterinary Medical Association*, **54**, 525-527. (In Japanese)

[7] Togashi, K. (1942) Morphological and Ecological Studies on the Ergot Fungus of *Zoysia japonica*. *Japanese Journal of Phytopathology*, **12**, 1-13. (In Japanese) https://doi.org/10.3186/jjphytopath.12.1

[8] Tanda, S. (1981) Mycological Studies on the Ergot in Japan. Part 20: *Claviceps yanagawaensis* Togashi Parasitic on Japonica STEUD. *J Agric Sci Tokyo Univ Agric*, **26**, 193-199. (In Japanese)

[9] Mulac, D., Lepski, S., Ebert, F., Schwerdtle, T. and Humpf, H.U. (2013) Cytotoxicity and Fluorescence Visualization of Ergot Alkaloids in Human Cell Lines. *Journal of Agricultural and Food Chemistry*, **61**, 462-471. https://doi.org/10.1021/jf304569q

[10] Doi, Y., Wakana, D., Takeda, H., Tanaka, E. and Hosoe, T. (2022) Production of Ergot Alkaloids by the Japanese Isolate *Claviceps purpurea* var. *agropyri* on Rice Medium. *Advances in Microbiology*, **12**, 254-269. https://doi.org/10.4236/aim.2022.124019

[11] Lv, J.M., *et al.* (2020) Biosynthesis of Biscognienyne B Involving a Cytochrome P450-Dependent Alkynylation. *Angewandte Chemie International Edition*, **59**, 13531-13536. https://doi.org/10.1002/anie.202004364

[12] Yamamoto, Y. (2010) The First General and Selective Palladium(II)-Catalyzed Alkoxycarbonylation of Arylboronates: Interplay among Benzoquinone-Ligated Palladium(0) Complex, Organoboron, and Alcohol Solvent. *Advanced Synthesis & Ca-*

talysis, **352**, 478-492. https://doi.org/10.1002/adsc.200900836

[13] Hothorn, T., Bretz, F. and Westfall, P. (2008) Simultaneous Inference in General Parametric Models. *Biometrical Journal*, **50**, 346-363. https://doi.org/10.1002/bimj.200810425

[14] Farooq, S., *et al.* (2020) Discovery of a Secalonic Acid Derivative from *Aspergillus aculeatus*, an Endophyte of *Rosa damascena* Mill., Triggers Apoptosis in MDA-MB-231 Triple Negative Breast Cancer Cells. *ACS Omega*, **5**, 24296-24310. https://doi.org/10.1021/acsomega.0c02505

[15] Steyn, P.S. (1970) The Isolation, Structure and Absolute Configuration of Secalonic Acid D, the Toxic Metabolite of *Penicillium oxalicum*. *Tetrahedron*, **26**, 51-57. https://doi.org/10.1016/0040-4020(70)85006-2

[16] Franck, B., Gottschalk, E., Ohnsorge, U. and Hüper, F. (1966) Mutterkorn-Farbstoffe, XII. Trennung, Struktur und Absolute Konfiguration der Diastereomeren Secalonsäuren A, B und C. *Chemische Berichte*, **99**, 3842-3862. https://doi.org/10.1002/cber.19660991218

[17] Lünne, F., *et al.* (2021) Insights into Ergochromes of the Plant Pathogen *Claviceps purpurea*. *Journal of Natural Products*, **84**, 2630-2643. https://doi.org/10.1021/acs.jnatprod.1c00264

[18] Chen, M., Gui, Y., Zhu, H., Zhang, Z. and Lin, H.W. (2019) Proangiogenic Penibishexahydroxanthone A from the Marine-Derived Fungus *Penicillium* sp. ZZ486A. *Tetrahedron Letters*, **60**, 1393-1396. https://doi.org/10.1016/j.tetlet.2019.04.034

[19] Wei, X. and Matsuda, Y. (2020) Unraveling the Fungal Strategy for Tetrahydroxanthone Biosynthesis and Diversification. *Organic Letters*, **22**, 1919-1923. https://doi.org/10.1021/acs.orglett.0c00285

[20] Wei, X., Wang, W.G. and Matsuda, Y. (2022) Branching and Converging Pathways in Fungal Natural Product Biosynthesis. *Fungal Biology and Biotechnology*, **9**, Article No. 6. https://doi.org/10.1186/s40694-022-00135-w

[21] Morris, R.A.C., Ewing, D.F., Whipps, J.M. and Coley-Smith, J.R. (1995) Antifungal Hydroxymethyl-Phenols from the Mycoparasite *Verticillium biguttatum*. *Phytochemistry*, **39**, 1043-1048. https://doi.org/10.1016/0031-9422(95)00165-4

[22] Neubauer, L., Dopstadt, J., Humpf, H.-U. and Tudzynski, P. (2016) Identification and Characterization of the Ergochrome Gene Cluster in the Plant Pathogenic Fungus *Claviceps purpurea*. *Fungal Biology and Biotechnology*, **3**, Article No. 2. https://doi.org/10.1186/s40694-016-0020-z

[23] Kurobane, I., Vining, L.C. and Gavin McInnes, A. (1979) Biosynthetic Relationships among the Secalonic Acids: Isolation of Emodin, Endocrocin and Secalonic Acids from *Pyrenochaeta terrestris* and *Aspergillus aculeatus*. *The Journal of Antibiotics*, **32**, 1256-1266. https://doi.org/10.7164/antibiotics.32.1256

[24] Wei, X., *et al.* (2021) Heterologous Biosynthesis of Tetrahydroxanthone Dimers: Determination of Key Factors for Selective or Divergent Synthesis. *Journal of Natural Products*, **84**, 1544-1549. https://doi.org/10.1021/acs.jnatprod.1c00022

[25] Franck, B. (1969) Structure and Biosynthesis of the Ergot Pigments. *Angewandte Chemie International Edition in English*, **8**, 251-260. https://doi.org/10.1002/anie.196902511

[26] Franck, B. and Baumann, G. (1966) Mutterkorn-Farbstoffe, XIV. Isolierung, Struktur und Absolute Konfiguration der Ergochrome AD, BD, CD und DD. *Chemische Berichte*, **99**, 3875-3883. https://doi.org/10.1002/cber.19660991220

[27] Flieger, M., *et al.* (2019) Ergochromes: Heretofore Neglected Side of Ergot Toxicity. *Toxins*, **11**, Article No. 439. https://doi.org/10.3390/toxins11080439

Supplementary

Table S1. NMR data for compound **3** and methyl bigutol in $CDCl_3$.

NMR data position	Compound **3**		Methyl bigutol	
	δ_C	δ_H (j in Hz)	δ_C	δ_H (j in Hz)
1	135.6		127.5	
2	146.3		143.0	
3	152.8		144.1	
4	108.9	6.81 (d, 2.1)	107.7	6.78 (d)
5	136.5		132.9	
6	120.2	6.75 (d, 1.37)	120.9	6.73 (d)
7	28.4	3.34 (d, 7.56)	28.2	3.36 (d)
8	122.8	5.26 (m)	122.2	5.31 (m)
9	132.4		132.2	
10	25.8	1.73 (brs)	25.9	1.73 (m)
11	17.8	1.72 (brs)	17.9	
12	65.4	4.60 (d, 5.5)	65.8	4.58 (s)
13	55.7	3.86 (s)	56.1	3.89 (s)
14	60.5	3.79 (s)		

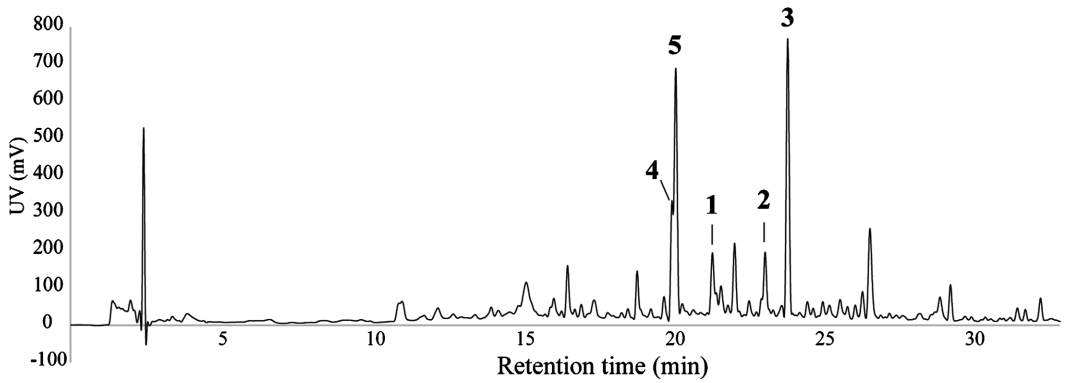

Figure S1. HPLC chromatogram (210 nm) of methanol extract of *C. yanagawaensis* rice culture.

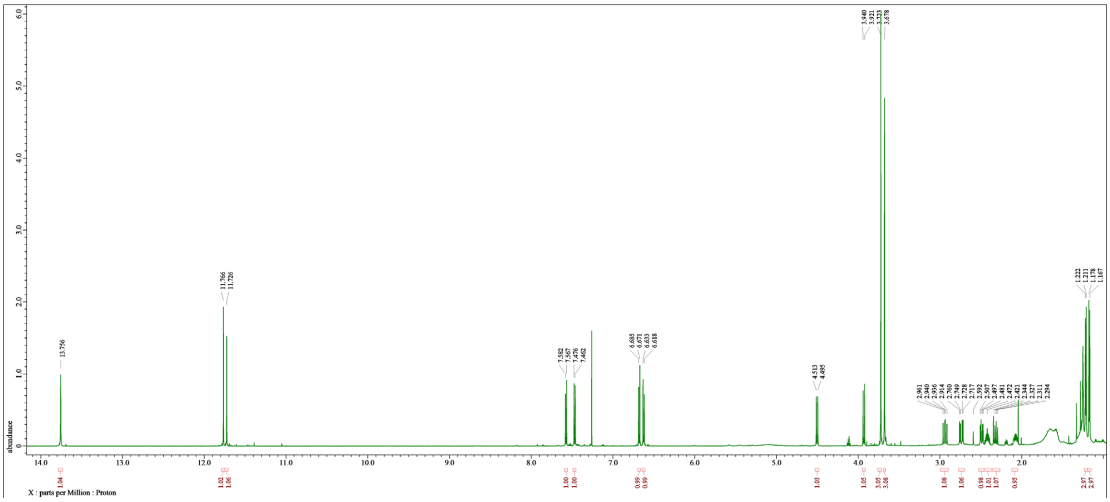

Figure S2. ^{1}H-NMR spectrum of **1** in $CDCl_3$.

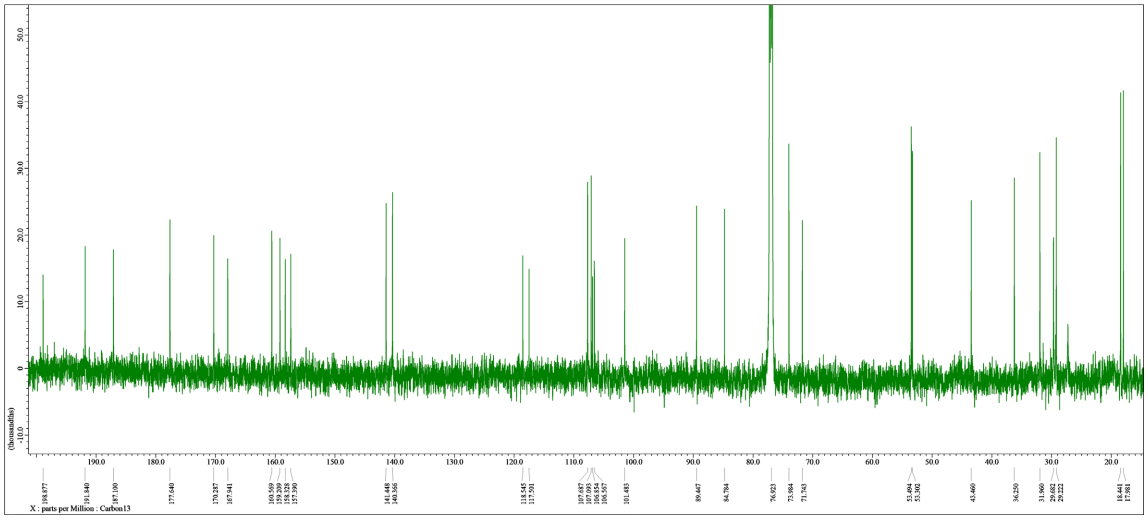

Figure S3. ^{13}C-NMR spectrum of **1** in $CDCl_3$.

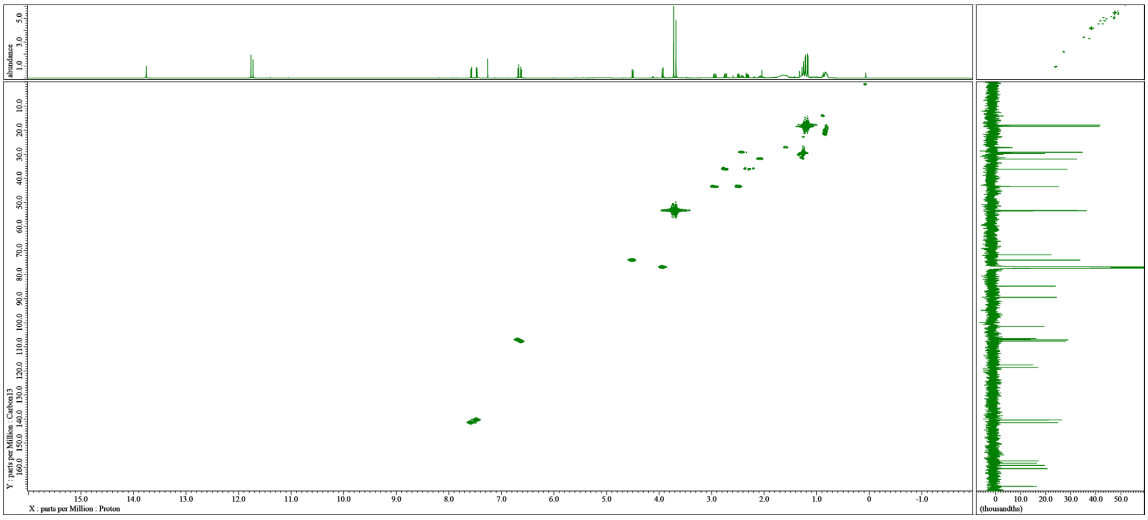

Figure S4. HMQC spectrum of **1** in $CDCl_3$.

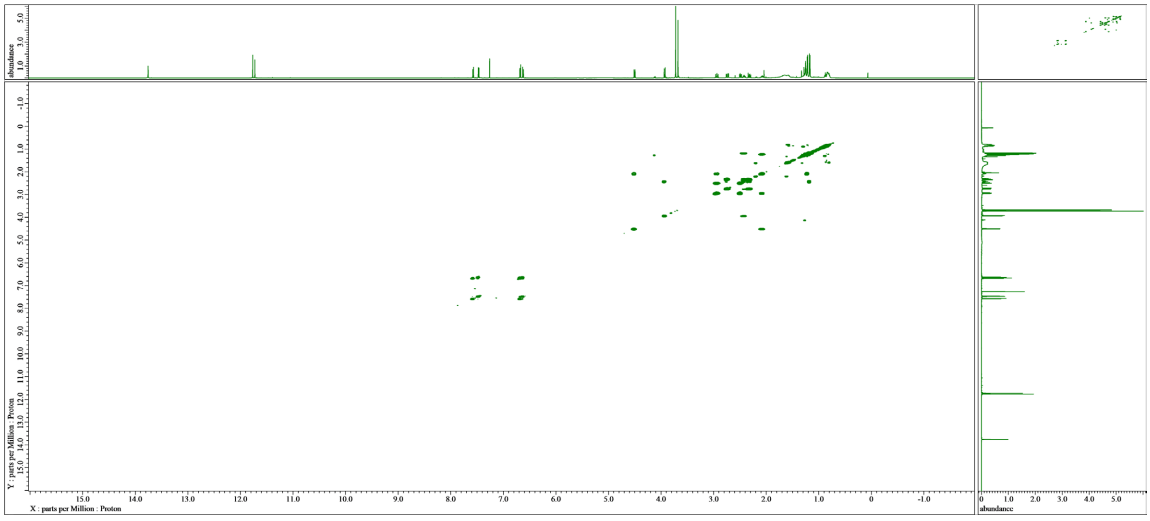

Figure S5. ^{1}H-^{1}H COSY spectrum of **1** in $CDCl_3$.

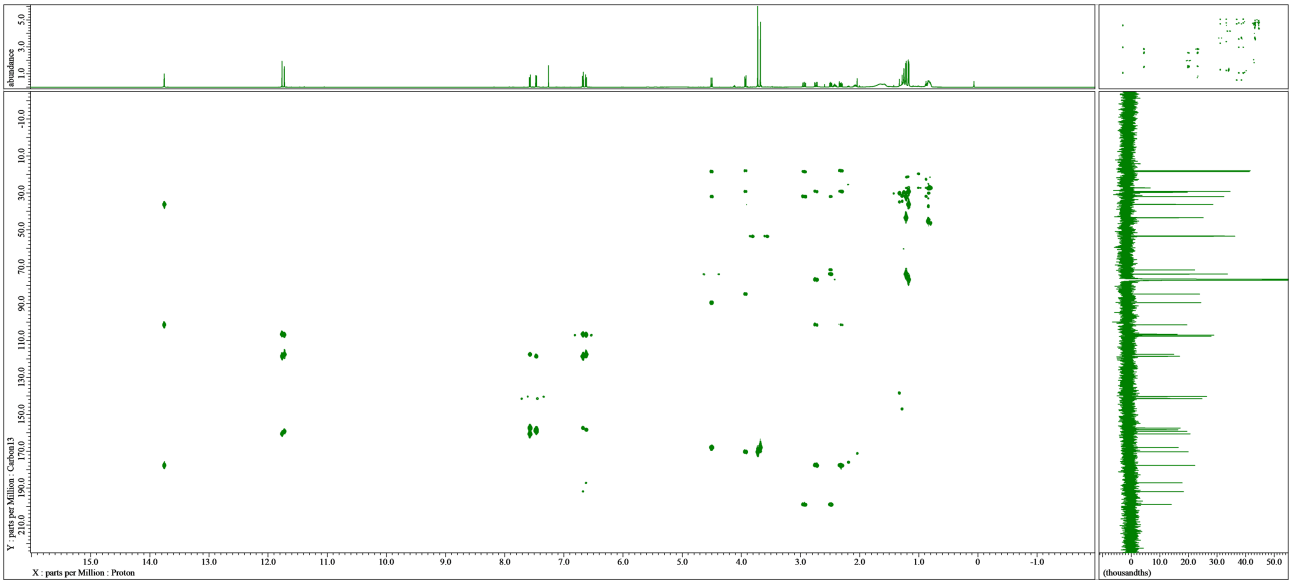

Figure S6. HMBC spectrum of **1** in $CDCl_3$.

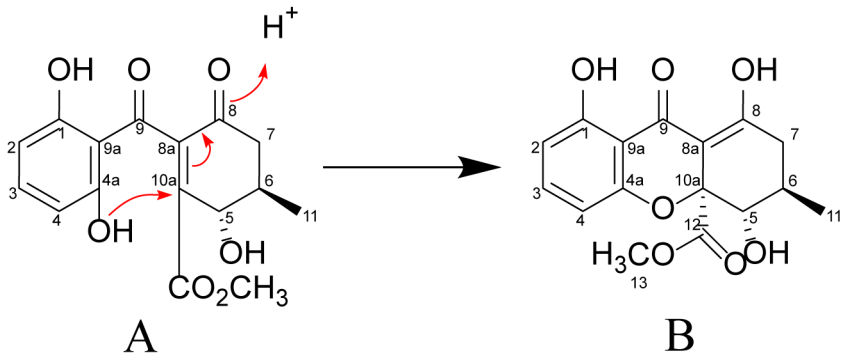

Figure S7. Spontaneous heterocyclization of hydroxycyclohexenones stereochemically controlled by 1,3-pseudoaxial interaction.

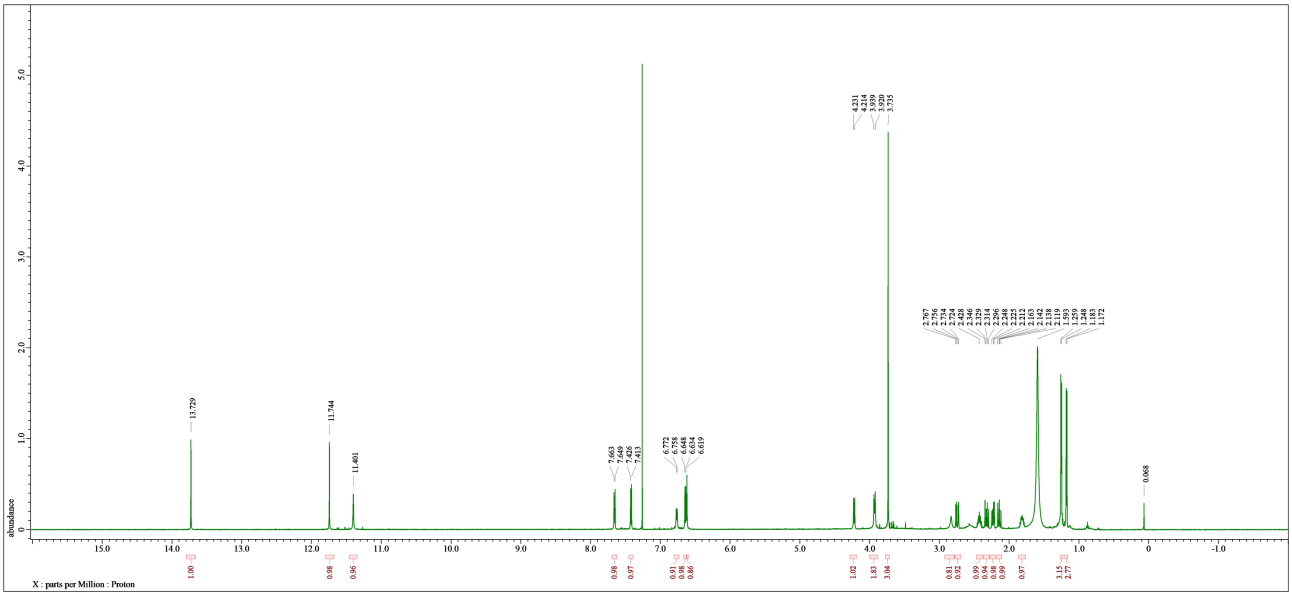

Figure S8. ^{1}H-NMR spectrum of **2** in $CDCl_3$.

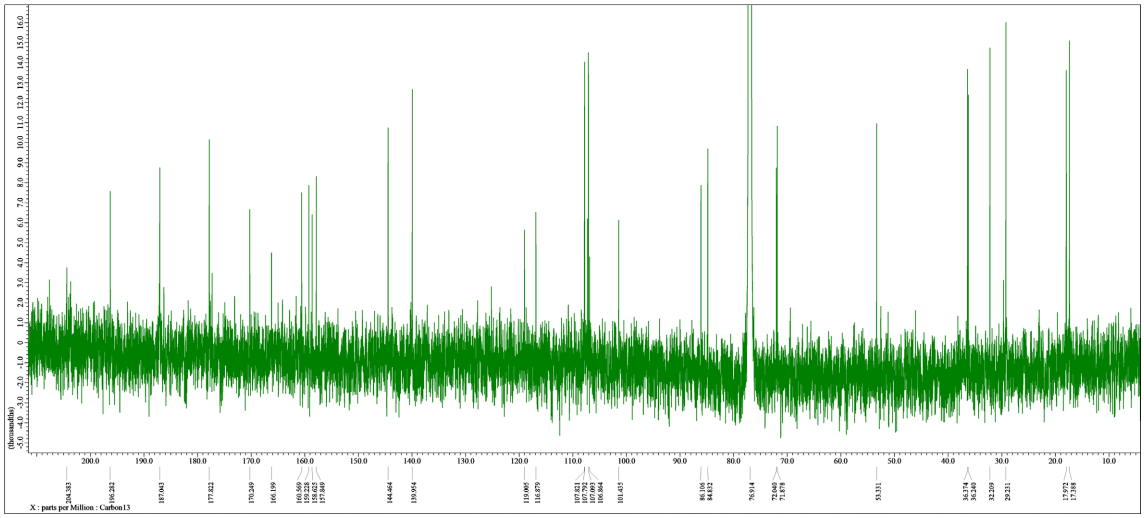

Figure S9. ^{13}C-NMR spectrum of **2** in $CDCl_3$.

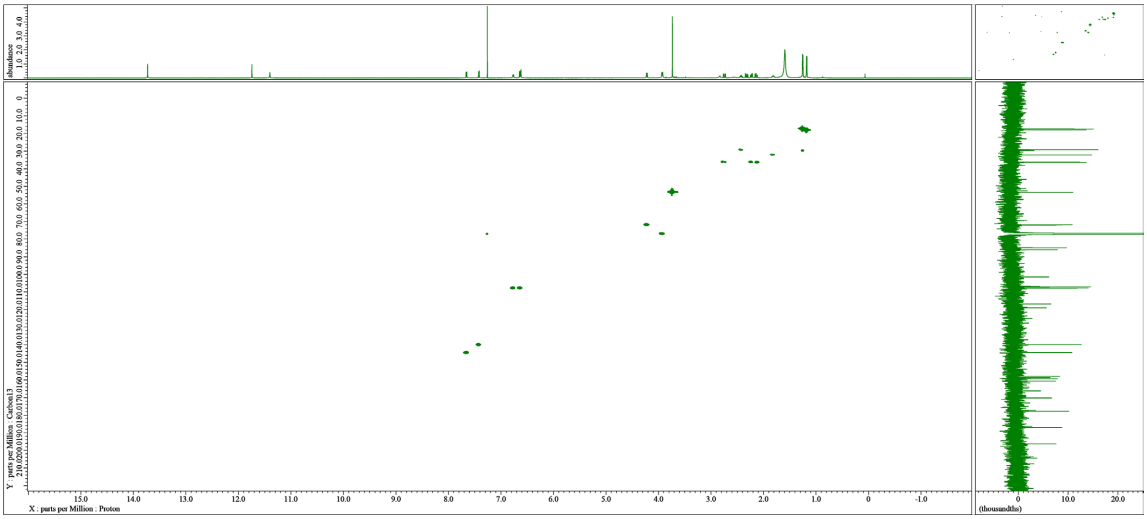

Figure S10. HMQC spectrum of **2** in $CDCl_3$.

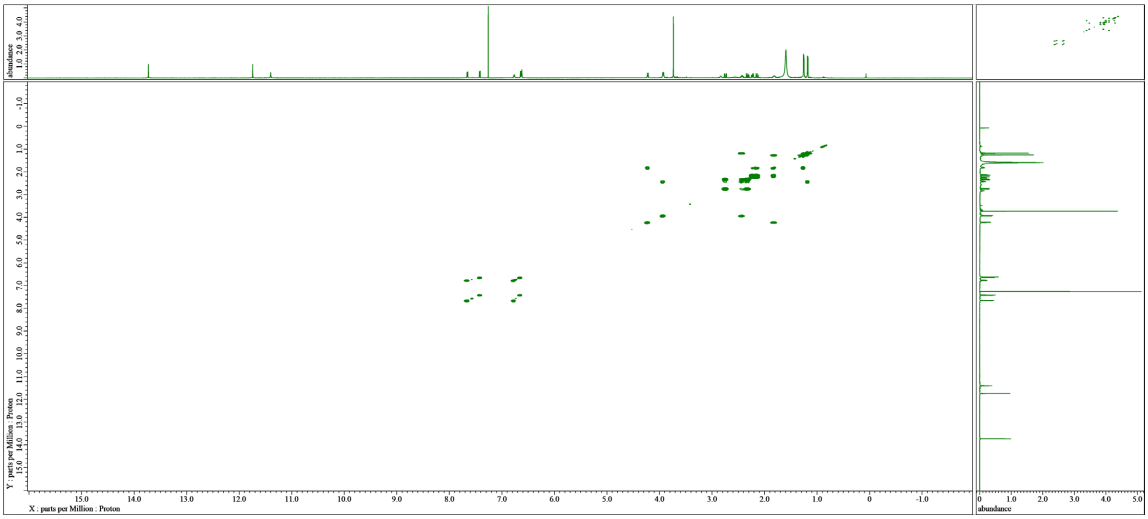

Figure S11. ^{1}H-^{1}H COSY spectrum of **2** in $CDCl_3$.

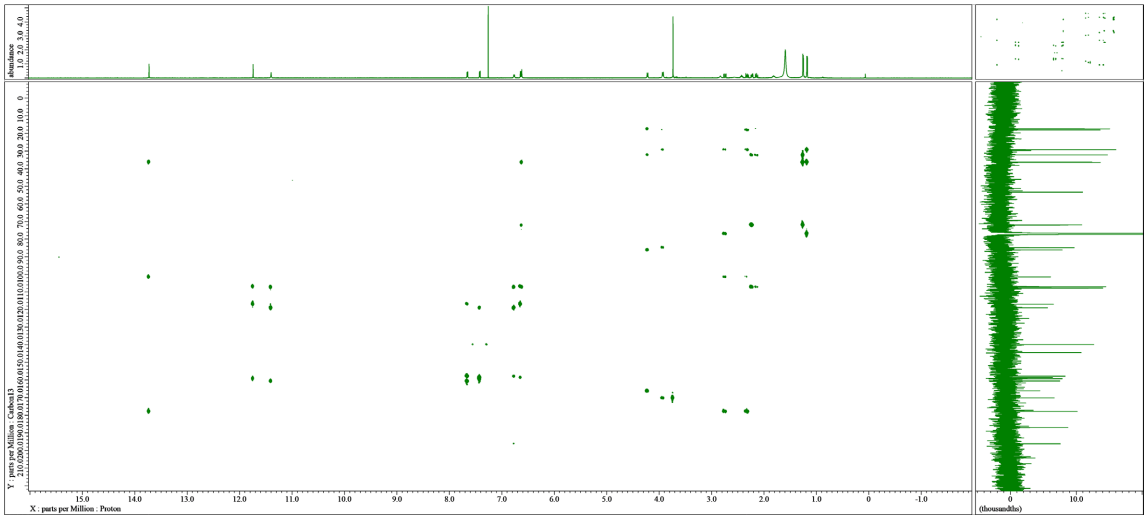

Figure S12. HMBC spectrum of **2** in $CDCl_3$.

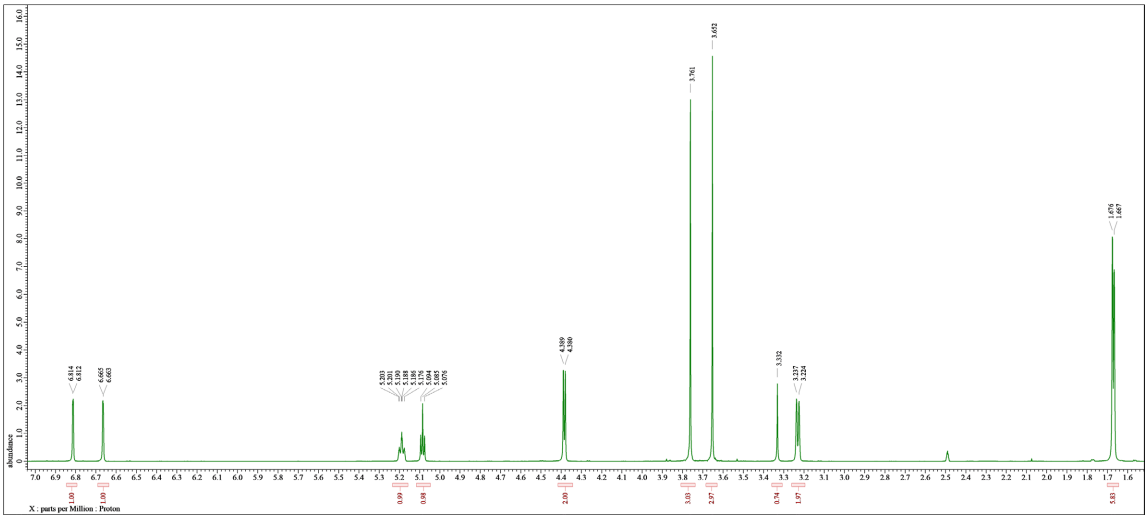

Figure S13. ^{1}H-NMR spectrum of **3** in DMSO-d_6.

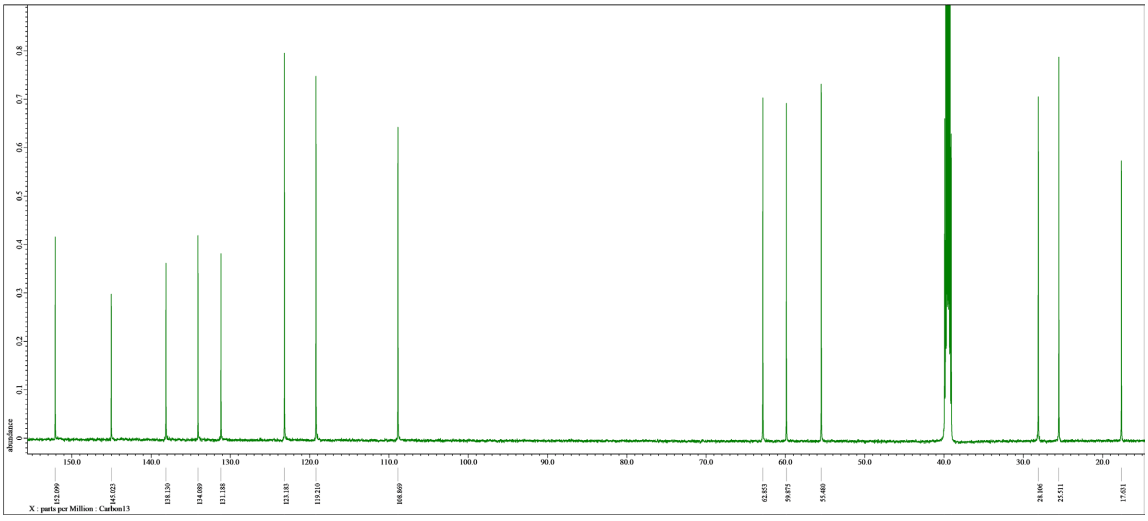

Figure S14. ^{13}C-NMR spectrum of **3** in DMSO-d_6.

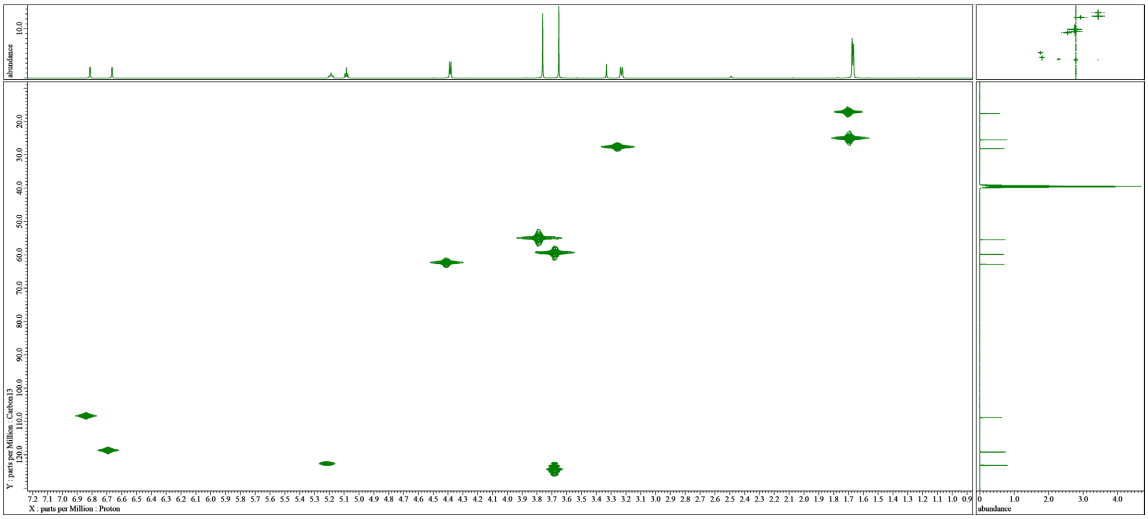

Figure S15. HMQC spectrum of **3** in DMSO-d_6.

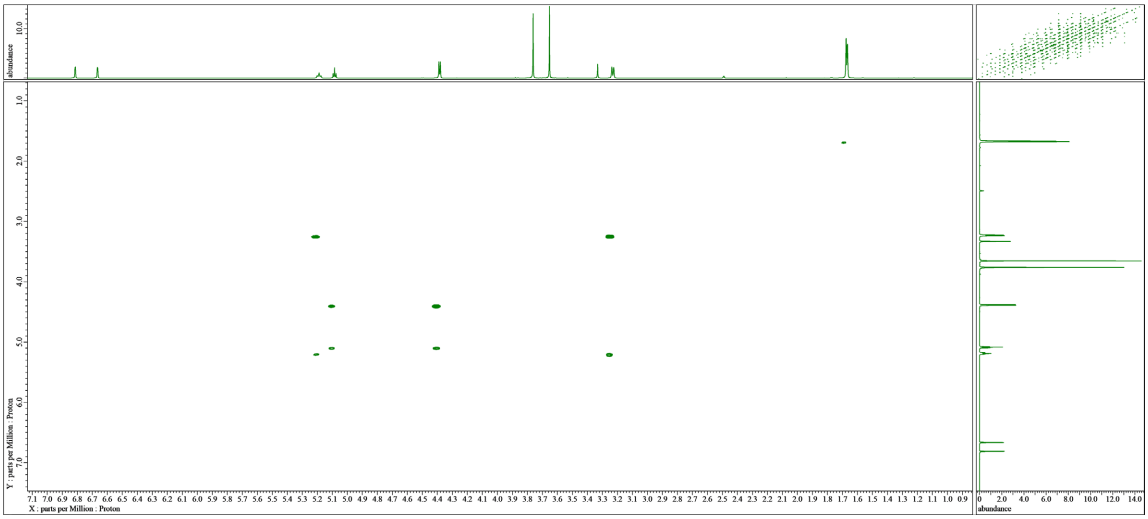

Figure S16. ^{1}H-^{1}H COSY spectrum of **3** in DMSO-d_6.

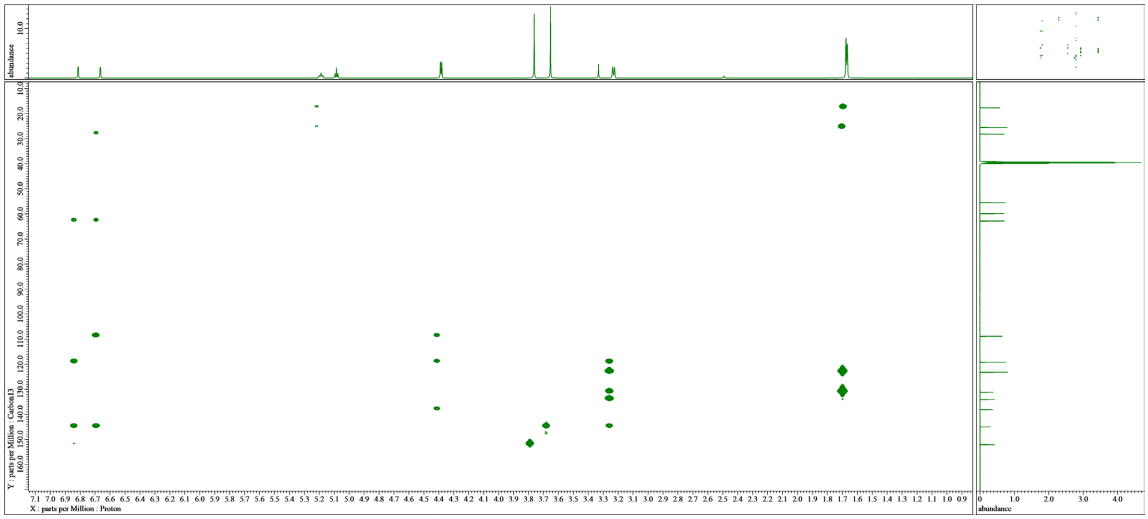

Figure S17. HMBC spectrum of **3** in DMSO-d_6.

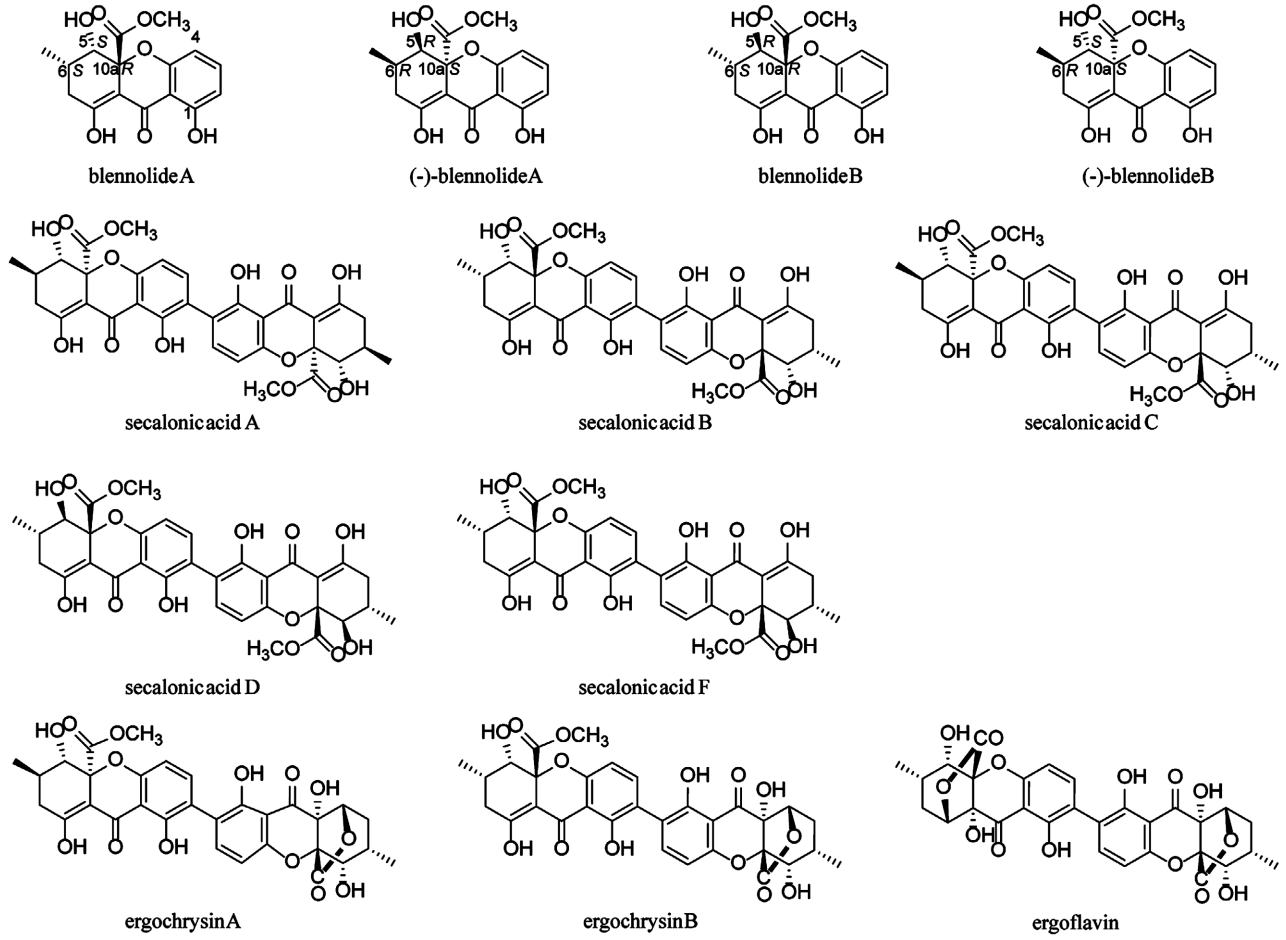

Figure S18. Structures of major secalonic acids and their monomers isolated from *Claviceps* and *Aspergillus*.

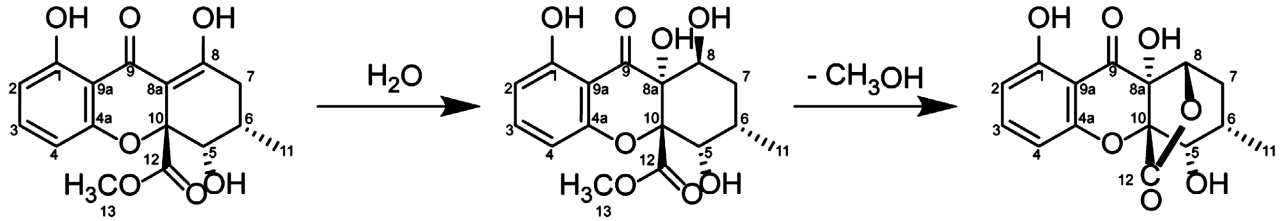

Figure S19. Predicted scheme of the lactonization of ergoflavin, ergochrysin A, and ergochrysin B [25].